Time-dependent electron tunneling through parabolic quantum wells

H. Cruz and J. G. Muga
Departamento de Física Fundamental y Experimental, Universidad de La Laguna, 38204 La Laguna, Tenerife, Spain
(Received 30 August 1991)

The time-dependent tunneling of electron wave packets through parabolic quantum wells is numerically studied. We consider both true smooth parabolic wells and quasiparabolic short-period superlattice potentials. The evolution of the charge density is described in detail. The electron dwell time at various resonance energies is also calculated.

In the past few years, resonant tunneling through quantum-well heterostructures has attracted considerable attention due to its possible applications to ultrahighspeed electronic devices.[1-6] In the fabrication of quantum wells, computer control of molecular-beam shutters has allowed very precise shaping of the potential through compositional grading.[7,8] Among the different profiles, parabolic quantum wells present the appealing feature of having equally spaced levels. Capasso and Kiehl proposed a resonant-tunneling bipolar transistor with a smooth parabolic well in the base layer, with the goal of achieving equally spaced peaks in the collector characteristics.[9] True parabolic (smooth) quantum wells are mimicked in practice through a set of GaAs-$Ga_{1-x}Al_xAs$ square quantum wells and barriers such that the electron potential, averaged over lengths longer than the individual well and barrier thicknesses, has a parabolic profile (Fig. 1). More specifically, the total width of the lattice is divided into a regularly spaced grid, each segment having one layer of GaAs (well) and one layer of $Ga_{1-x}Al_xAs$ (barrier). The barrier thickness is varied quadratically with the distance from the center of the superlattice, while the height, determined by x, is kept constant. The averaged potential of the short-period (SP) superlattices is expected to be the effective electron potential if the electron wave function extends over many of the individual wells and barriers.[10,11] Quasiparabolic wells grown by molecular-beam epitaxy (MBE) exhibited the expected nearly equally spaced transitions in the photoluminescence[8] and light-scattering spectra.[10] The observation of resonances in a compositionally graded parabolic quantum well has been reported by Sen *et al.*[12] These parabolic quantum wells [Fig. 1(b)], used as a resonant-tunneling device, exhibited equally spaced peaks in the collector characteristics[12] in reasonable agreement with the theoretical results obtained through a smooth parabolic potential [Fig. 1(a)] in a stationary scheme, solving analytically the one-dimensional effective-mass equation by means of confluent hypergeometric functions.[13]

While mainly static features of the tunneling phenomena have been investigated, dynamical aspects have not been studied thoroughly. This is in part because the characteristic time scale of the process is typically of the order of picoseconds or less, which is shorter than the measurable time by commonly available methods. Numerical methods are also difficult to apply, especially when two or more degrees of freedom have to be considered. Nevertheless, dynamics should be investigated, since it not only determines the ultimate speed of tunneling devices, but it elucidates fundamental aspects of electronic waves in solids, particularly their behavior in the time domain.[14,15] Experimental progress is being made in the measuring of tunneling escape times.[16] (The tunneling escape time of electrons from parabolic quantum wells in double barrier heterostructures has been calculated recently by means of a transfer-matrix method in a stationary scheme.[17]) On the computational side, efficient grid methods are also being implemented. Ancilotto, Selloni, and Tosatti,[18] have recently studied the time-dependent resonant electron tunneling through double barrier heterostructures.

Our aim here is to compare the single-electron-wave-packet dynamics in the true parabolic potential V_p, and in the superlattice quasiparabolic structure V_q. Differences can be expected, because even if the average of the two potentials (over one period or more) agrees, averaged forces $-\partial V/\partial z$ and higher derivatives of V will

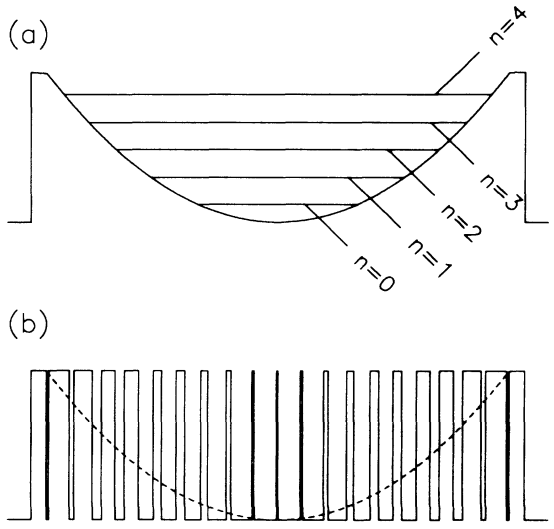

FIG. 1. Parabolic quantum well in a double barrier heterostructure. (a) Smooth parabolic potential with the different energy levels. (b) The equivalent parabolic potential (dashed line) achieved through a short-period superlattice with $N=19$.

be different in general: the square barrier superlattice model potential can be mathematically regarded as a combination of Heaviside functions with appropriate arguments. Its derivative is then either zero in wells and barriers or plus or minus a δ function in the limits between them (*plus* at the left edge of the barriers, *minus* at the right edges). A more realistic version with smoothed edges keeping the main features of the square barrier model does not essentially modify our reasoning. Since the derivatives of V determine the time evolution, as is made explicit in the evolution equation for the Wigner function W,

$$\frac{\partial W}{\partial t}=-\frac{\partial W}{\partial z}\frac{p}{m}+\sum_{n\ \text{odd}}\frac{(i\hbar)^{n-1}}{2^{n-1}n!}\left[\frac{\partial}{\partial p}\frac{\partial}{\partial z}\right]^n VW\ , \tag{1}$$

a dynamical disagreement seems possible. The simplest type of dynamical information is contained in the Hamilton-like Ehrenfest-theorem equations. In particular, the evolution of the average momentum is given by

$$\frac{d\langle p\rangle}{dt}=\left\langle -\frac{\partial V}{\partial z}\right\rangle\ , \tag{2}$$

where the brackets stand for the quantum-mechanical average over the wave function $\psi(z)$. An explicit expression can actually be obtained for the superlattice in terms of the various δ-function contributions:

$$\begin{aligned}\left\langle -\frac{\partial V_q}{\partial z}\right\rangle&=\int -\frac{\partial V}{\partial z}|\psi(z)|^2dz\\&=-c\sum_n(-1)^{s(n)}|\psi(z_n)|^2\\&=-c\sum_k[|\psi(z_k^l)|^2-|\psi(z_k^r)|^2]\ .\end{aligned} \tag{3}$$

Here c is a constant determined by the number of barriers and the barrier height, and the first sum runs over the singularities at points z_n. $s(n)$ is zero for left barrier edges and one for right barrier edges. The second sum runs over superlattice periods centered at points z_k. Every period gives a positive and a negative contribution coming from the left and right barrier edges (z_k^l and z_k^r). The above discretized (but exact) expression can be compared with the discretized approximation of the corresponding integral for the smooth parabolic potential

$$\langle -\partial V_p/\partial z\rangle=-2\delta\sum_l z_l|\psi(z_l)|^2\ , \tag{4}$$

where for simplicity $V_p=z^2$ is assumed, and δ is the superlattice period, taken here as the elementary discretization length. The two expressions do not much resemble each other for arbitrary densities $|\psi|^2$, although they may give similar results for particular cases.

Another way to understand the origin of a difference between the dynamics in the two potentials is to notice that while the motion in a smooth parabolic potential is purely classical (the terms depending on $\hbar^2$ or higher orders vanish in the Wigner equation giving the classical Liouville equation), discontinuous potentials are one of the sources of classical–quantum-mechanical disagreement.[19,20]

From a different perspective, the small deviations between the spectra of the smooth parabolic potential and the superlattice that have been calculated and found experimentally[10] suggest again that different dynamical responses could be encountered, since the dynamics are ultimately determined by the stationary eigenvalues and eigenfunctions.

The question then is what is the quantitative importance of this effect. Our numerical study provides an answer. In this work, we have found that the electron dwell time for a parabolic quantum well achieved by means of a SP superlattice takes a different value than that expected from the smooth parabolic potential calculation. The dwell time depends on the period chosen for the superlattice. This period will be given by the number of barriers N taken in the fixed quantum-well width [Fig. 1(b)]. The detailed wave-packet motion is also examined.

The simplest way to describe electron tunneling through a double barrier heterostructure (DBH) is the effective-mass approach.[21] We have assumed the same effective mass inside and outside the barrier regions: $m^*=0.067m_0$, where $m_0=1$ in atomic units.

Our heterostructures are formed by a $2L=300$ Å parabolic (or quasiparabolic) quantum well sandwiched between two $d=10$ Å $Ga_{1-x}Al_xAs$ barriers of $V=0.27$ eV height. The smooth parabolic quantum well is depicted in Fig. 1(a) where the quadratic part is given by $V_p(z)=(V/L^2)z^2$ where $2L$ is the parabolic well width. In Fig. 1(b), the SP $Ga_{1-x}Al_xAs$ superlattice, in which the Al content with each period is varied such that the averaged electron potential has a parabolic profile [dashed line in Fig. 1(b)], is represented.[12]

In order to study the dynamics of tunneling, we need to solve the time-dependent Schrödinger equation associated with the Hamiltonian for a spinless electron in the heterostructure region

$$H=-(\hbar^2/2m^*)\partial^2/\partial z^2+V_{\mathrm{PQW}}(z)\ , \tag{5}$$

where $V_{\mathrm{PQW}}(z)$ represents the quantum-well potentials of Fig. 1. Recently, a large amount of dynamical simulations of quantum systems using grid methods have been performed in different fields.[22–24] The wave function is discretized first at time $t=0$ on a spatial grid. Then, a propagation algorithm transforms the initial wave function $\psi(t=0)$ into the final one $\psi(t)$. The work by Ancilotto, Selloni, and Tosatti is based on a Chebychev scheme for the time evolution operator[18] in combination with fast Fourier transform (FFT) techniques. The efficiency of this type of numerical method for two or more dimensions has been repeatedly proved. However, for one-dimensional problems, other methods become faster and easier to implement.[23] We have used Koonin's method.[25] This is also a grid method based on the following unitary propagator scheme:

$$\psi^{n+1}=\left[\frac{1-iH\,\Delta t/2}{1+iH\,\Delta t/2}\right]\psi^n\ , \tag{6}$$

where ψ^n is the wave function at the time step n. The initial state is taken as usual as a Gaussian packet

$$\psi(0)=(2\pi\sigma)^{-1/4}e^{-(z-z_0)^2/4\sigma}e^{ik_0z} . \quad (7)$$

σ is the spatial width of the wave packet, z_0 the initial average position, and $k_0\hbar$ its initial average momentum. The spatial width of the packet has been chosen large enough to avoid an excessive smoothing of the stationary transmittance features due to a wide momentum distribution. In a recent article,[19] a quantitative analysis of this phenomenon in terms of dimensionless quantities has been given. In summary, for a fixed value of the average energy of the packet, a wide momentum distribution destroys the quantum resonance features and makes the quantum-mechanical results closer to the classical ones, obtained from an ensemble of classical particles.

Let us discretize time by a superscript n and spatial position by a subscript j. Thus $\psi(z,t)\rightarrow\psi_j^n$. The various z values become $j\,\Delta z$ where Δz is the mesh width. Similarly, the time variable goes over to $n\,\Delta t$ where Δt is the time step. The second spatial derivative is approximated as

$$\psi_j''=[1/(\Delta z)^2](\psi_{j+1}-2\psi_j+\psi_{j-1})+O((\Delta z)^2) . \quad (8)$$

To treat the time development of $\psi(z,t)$, we use the unitary propagation scheme[24] given in Eq. (5). This norm conserving algorithm approximates the exact evolution operator through second order in Δt. For a practical application (5) is rewritten as $\psi^{n+1}=\chi-\psi^n$, where χ satisfies

$$(1+iH\,\Delta t/2)\chi=2\psi^n . \quad (9)$$

The spatial discretization of the preceding equation leads to a tridiagonal linear system that can be solved by standard methods.

Let us consider the electron tunneling through a parabolic quantum well. Particle transmission can exhibit sharp peaks when the incident particle energy coincides with the energies of the quasibound states of the quantum well, and the thickness of the confining barriers affects mainly the width of the peak, the latter being related to the lifetime to escape out of the well.[17] In a parabolic quantum well, in the absence of an external applied electric field, the electron energy levels are given by

$$E_n\approx\hbar\omega_p(n+\tfrac{1}{2}) , \quad (10)$$

where $n=0,1,2,\ldots$ and $\omega_p=(2V/mL^2)^{1/2}$. These levels are nearly equally spaced and from (10) the spacing ΔE between states is $\Delta E\approx\hbar\omega_p$ [Fig. 1(a)]. Equation (10) is not exact because, in our case, the parabolic potential is not infinite and the eigenfunctions are not exact Hermite polynomials.[11] When an external electric field is applied to a parabolic quantum well, it preserves the curvature of the parabola, and therefore the energy levels and the spacing ΔE, while shifting its origin to the right.[12] In this work, we will not consider an applied electric field to establish a tunneling current through the heterostructure. We will vary the incident energy of the particle as in Ref. 18.

In Fig. 2, the evolution of a packet initially characterized by a width $\sigma=230$ Å, $0.81V_0$ total energy, and localized on the left of Fig. 1(a) is shown as a sequence of plots

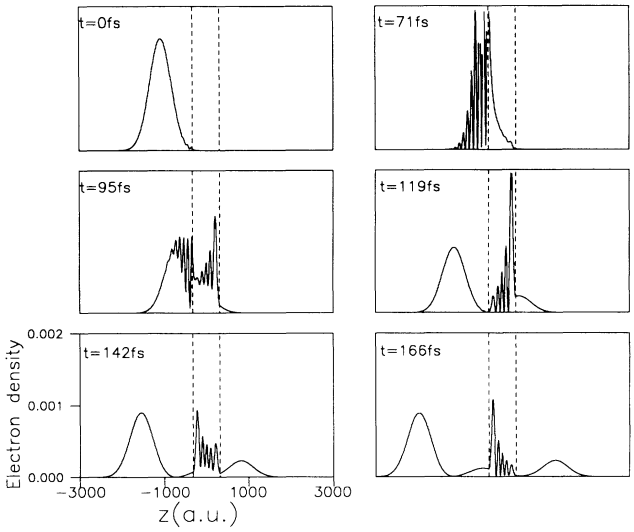

FIG. 2. Evolution of the electron wave packet in the tunnel through Fig. 1(a) potential. The dashed line represents the heterostructure position.

of the charge density $|\psi(z,t)|^2$ at $n=4$ resonance in the parabolic quantum well versus z (in a.u.). A spatial grid with side $L=6000$ a.u. and 6000 points has been used; the time step was taken as 10 a.u. This grid provides converged results and allows us safely to neglect boundary effects. It can be seen that an interference pattern is formed due to the intertwining of reflected and ingoing fluxes. A part of the electron wave packet enters between the barriers, giving a series of peaks of the charge density that bounce back and forth between the parabolic quantum-well edges, where reflected and transmitted packets are produced by tunneling. (The dashed line represents the position of the heterostructure.)

We plot in Fig. 3 the charge density versus z (in a.u.) at various times at $n=4$ resonance for the smooth parabolic well and for different N values of the quasiparabolic superlattice ($N=15,19$). The entrance of the charge within a smooth parabolic quantum well can be emulated in a very good manner by means of a SP superlattice, but when the charge trapped between the barriers grows to a maximum and then starts to decay, differences are found between the electron wave functions for the different heterostructure potentials. Specifically, the phase of the oscillatory pattern of the charge density is different in both cases. This is more evident in Fig. 3 at $t=143$ fs.

In Figs. 2 and 3, one can observe that the charge density trapped in the parabolic well grows in a "charge time" up to a maximum and then slowly decays.

In Fig. 4, we have plotted $Q(t)=\int_a^b|\psi|^2dz$ versus time for the cases described, a and b being the parabolic well limits. The features of $Q(t)$ in the scattering process are related to two phenomena that occur simultaneously, at least for an intermediate time period between the beginning and the end of the collision: a charge process due to the incoming wave and a decay due to the like barriers modulated by the bouncing of the packet between the

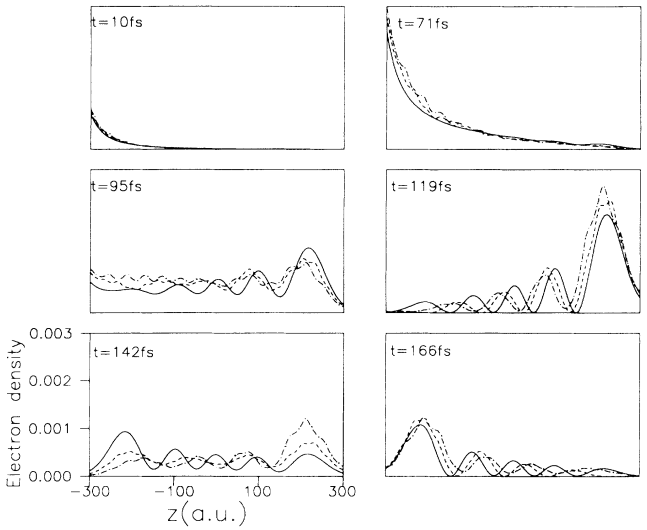

FIG. 3. Evolution of the electron wave functions within the parabolic quantum well in the resonant-tunneling process. Solid line, Fig. 1(a) potential; dashed line, short-period superlattice with $N=19$; dot-dashed line, short-period superlattice with $N=15$.

well edges. The charge process due to the incoming wave can be reproduced by means of a SP superlattice in reasonable agreement with a smooth parabolic quantum well if we take a large value for N, $N=15$ or $N=19$ in Fig. 4, although the charge maximum in the well is always higher for the SP superlattice than for the smooth parabolic potential case. This can be attributed to the short left barrier in the SP superlattice that favors the entrance of charge within the parabolic well. If N is not large enough ($N=11$ in Fig. 4) the electron potential, averaged over lengths not longer than the well and barrier thickness in the SP superlattice, does not have a parabolic profile. In this case, the charge process is very different and the charge maximum in the well (dot-dashed line in Fig. 4) takes a lower value than in the smooth parabolic case due to the loss of the resonant state within the barriers. From now on, we will only consider the cases $N=15$ and 19 in our calculations.

With respect to the decay process, it is qualitatively similar in the smooth parabolic or superlattice potentials. However, the detailed oscillations take different phases in both cases. This should not be surprising, as the packet has had enough time to sense the sharp interfaces in the superlattice.

Apart from the calculation of charge densities, we have evaluated the dwell time τ_D,

$$\tau_D(a,b,t_1,t_2)=\int_{t_1}^{t_2}dt\int_a^b dz|\psi(z,t)|^2 . \tag{11}$$

When $t_1=-\infty$ and $t_2=\infty$, τ is interpreted as the average of the time spent by the electron in the well region,[26] $a<b$. In an actual computation, the integral over t in (11) is performed from $t_1=0$ (when no charge is present in the well) until certain value t_2 such that τ_D remains unchanged (the charge has been completely depleted from the well).

Important differences in the calculated dwell times for the potentials depicted in Fig. 4 are obtained. In Fig. 5, we have plotted the calculated electron dwell times at each n resonance in the parabolic quantum well for the different cases, τ_D for a SP superlattice with an $N=15,19$ value is higher than the smooth parabolic case. A 15–20% difference from the smooth parabolic case with the $N=19$ SP superlattice is found, and a 30–35% difference for $N=15$. The SP superlattice gives an extra multibarrier-induced dwell time for the charge trapped between the barriers at resonance. The study of larger values of N is not required because the parabolic quan-

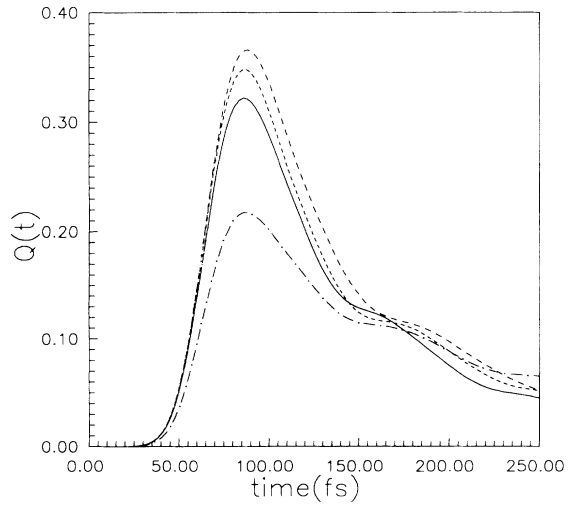

FIG. 4. Charge trapped between the barriers vs time. Solid line, Fig. 1(a) case; short dashed line, $N=19$; long dashed line, $N=15$; dotted-dashed line, $N=11$.

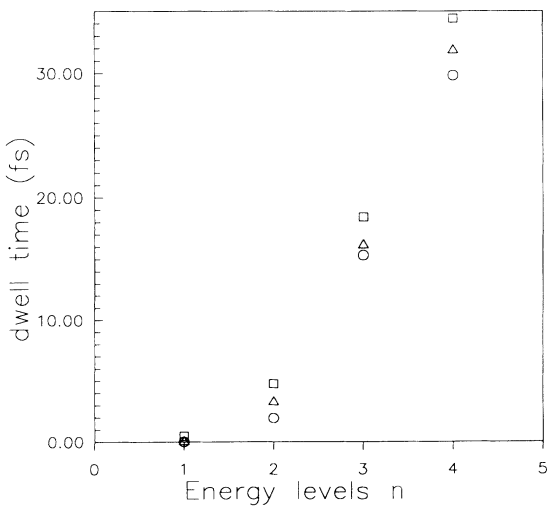

FIG. 5. Electron dwell time vs n (energy level). Circles, smooth parabolic potential; triangles, $N=19$ SP superlattice potential; squares, $N=15$ SP superlattice potential.

tum well achieved with $N=19$ already involves barrier thickness of 3-Å width in the center of the well. These short wide barriers cannot be produced within the actual GaAs-$Ga_{1-x}Al_xAs$ technology, so that at least a 30% difference in the dwell time is expected for a resonant-tunneling bipolar transistor with a parabolic well in the base layer.

In summary, we have studied the time evolution of the charge density of electron wave packets through parabolic quantum wells, and calculated the dwell time of the charge trapped between the two barriers in the parabolic well region. A resonant-tunneling bipolar transistor, with a parabolic well in the base layer achieved through a SP superlattice, has exhibited equally spaced peaks in the collector characteristics[18] in a good agreement with the proposed smooth parabolic potential,[11] but in this work we have found that it gives a dwell time at least 30% higher than the one obtained through the proposed smooth parabolic potential.

This work has been supported in part by Gobierno Autónomo de Canarias. One of us (J.G.M.) acknowledges the kind hospitality of Professor R. F. Snider at the University of British Columbia.

[1]E. R. Brown, T. C. L. G. Sollner, W. D. Goodhue, and C. D. Parker, Appl. Phys. Lett. **50**, 83 (1987).
[2]A. R. Bonnefoi, T. C. McGill, R. D. Burnham, and G. B. Anderson, Appl. Phys. Lett. **50**, 344 (1987).
[3]T. H. Wong, D. C. Tsui, and W. T. Tsang, Appl. Phys. Lett. **50**, 1004 (1987).
[4]M. A. Reed and J. W. Lee, Appl. Phys. Lett. **50**, 845 (1987).
[5]E. E. Mendez, W. I. Wang, E. Calleja, and C. E. T. Goncalves da Silva, Appl. Phys. Lett. **50**, 1263 (1987).
[6]H. Cruz, A. Hernández-Cabrera, and P. Aceituno, J. Phys. Condens. Mater. **6**, 8953 (1990).
[7]M. Kabawe, M. Kondo, N. Matsuura, and K. Yamamoto, Jpn. J. Appl. Phys. **22**, L64 (1983).
[8]R. C. Miller, A. C. Gossard, D. A. Kleinman, and O. Muntenau, Phys. Rev. B **29**, 3740 (1984).
[9]F. Capasso and R. A. Kiehl, J. Appl. Phys. **58**, 1366 (1985).
[10]J. Menendez, A. Pinczuk, A. C. Gossard, M. G. Lamont, and F. Cerdeira, Solid State Commun. **61**, 601 (1987).
[11]A. C. Gossard, R. C. Miller, and W. Wiegmann, Surf. Sci. **174**, 131 (1986).
[12]S. Sen, F. Capasso, A. C. Gossard, R. A. Spah, A. L. Hutchinson, and S. N. G. Chu, Appl. Phys. Lett. **51**, 1428 (1987).
[13]H. Cruz, A. Hernández-Cabrera, and A. Munoz, Semicond. Sci. Technol. **6**, 218 (1991).
[14]H. Cruz, A. Hernández-Cabrera, and P. Aceituno, Mod. Phys. Lett. B **4**, 1341 (1990).
[15]B. Deveaud, A. Chomette, F. Clerot, P. Auvray, A. Regreny, R. Ferreira, and G. Bastard, Phys. Rev. B **42**, 7021 (1990).
[16]M. Tsuchiya, T. Matsusue, and H. Sakaki, Phys. Rev. Lett. **59**, 2356 (1987).
[17]H. Cruz, A. Hernández-Cabrera, and A. Munoz, Mod. Phys. Lett. B **5**, 293 (1991).
[18]F. Ancilotto, A. Selloni, and E. Tosatti, Phys. Rev. B **40**, 3729 (1989).
[19]J. G. Muga, J. Phys. A **24**, 2003 (1991).
[20]P. A. Markowich, A. Ringhofer, and C. Scmeiser, *Semiconductor Equations* (Springer-Verlag, Berlin, 1990).
[21]R. Tsu and L. Esaki, Appl. Phys. Lett. **22**, 562 (1973).
[22]R. B. Gerber, R. Kosloff, and R. Berman, Comput. Phys. **5**, 59 (1986).
[23]R. Kosloff, J. Phys. Chem. **92**, 2087 (1988).
[24]A. D. Hammerich, J. G. Muga, and R. Kossloff, Isr. J. Chem. **29**, 461 (1989).
[25]S. E. Koonin, *Computational Physics* (Benjamin, Menlo Park, NJ, 1985).
[26]W. Jaworski and D. M. Wardlaw, Phys. Rev. A **37**, 2843 (1988).